Tellus
SERIES B
CHEMICAL
AND PHYSICAL
METEOROLOGY
PUBLISHED BY THE INTERNATIONAL METEOROLOGICAL INSTITUTE IN STOCKHOLM

Tellus (2010), 62B, 621–635
Printed in Singapore. All rights reserved

Rapid changes in surface water carbonate chemistry during Antarctic sea ice melt

By ELIZABETH M. JONES[1]*, DOROTHEE C. E. BAKKER[1], HUGH J. VENABLES[2], MICHAEL J. WHITEHOUSE[2], REBECCA E. KORB[2] and ANDREW J. WATSON[1], [1]*School of Environmental Sciences, University of East Anglia, Norwich NR4 7TJ, UK;* [2]*British Antarctic Survey, High Cross, Madingley Road, Cambridge CB3 0ET, UK*

(Manuscript received 18 December 2009; in final form 8 July 2010)

ABSTRACT

The effect of sea ice melt on the carbonate chemistry of surface waters in the Weddell–Scotia Confluence, Southern Ocean, was investigated during January 2008. Contrasting concentrations of dissolved inorganic carbon (DIC), total alkalinity (TA) and the fugacity of carbon dioxide (fCO_2) were observed in and around the receding sea ice edge. The precipitation of carbonate minerals such as ikaite ($CaCO_3{\cdot}6H_2O$) in sea ice brine has the net effect of decreasing DIC and TA and increasing the fCO_2 in the brine. Deficits in DIC up to 12 ± 3 μmol kg^{-1} in the marginal ice zone (MIZ) were consistent with the release of DIC-poor brines to surface waters during sea ice melt. Biological utilization of carbon was the dominant processes and accounted for 41 ± 1 μmol kg^{-1} of the summer DIC deficit. The data suggest that the combined effects of biological carbon uptake and the precipitation of carbonates created substantial undersaturation in fCO_2 of 95 μatm in the MIZ during summer sea ice melt. Further work is required to improve the understanding of ikaite chemistry in Antarctic sea ice and its importance for the sea ice carbon pump.

1. Introduction

The Southern Ocean greatly influences the climate system through the biological and physical pumps that facilitate the uptake of atmospheric carbon dioxide (CO_2) and transport of carbon to the deep ocean (Heinze et al., 1991). Marginal ice zones (MIZ) form the boundary from dense sea ice cover to the open ocean and show large spatial and temporal variability in sea surface CO_2 (Bakker et al., 1997; Gibson and Trull, 1999; Hoppema et al., 1999; Hoppema et al., 2000; Alvarez et al., 2002; Bellerby et al., 2004; Shim et al., 2006). The significance of sea ice regions in the oceanic carbon cycle has been demonstrated by a dramatic revision of the Southern Ocean (50–62°S) CO_2 sink estimate, from -0.34 to -0.06 Pg C yr^{-1} in the reference years 1995 and 2000, respectively (Takahashi et al., 2009). This trend has been governed by increased data coverage that highlights the dominance of winter CO_2 release, as a result of upwelling and respiration, over CO_2 uptake upon seasonal sea ice melt.

The eastward-flowing Antarctic Circumpolar Current (ACC) transports heat and dissolved constituents around the Antarctic continent (Rintoul and Sokolov, 2001). The dominant water mass in the ACC is Circumpolar Deep Water (CDW), a broad layer of warm, saline and nutrient-rich water, which shoals to the south with the uplifting isopycnals at the Southern Boundary (SB; Sievers and Nowlin, 1984; Orsi et al., 1995; Pollard et al., 2002).

The Weddell Sea is dominated by a cyclonic gyre, bounded to the west and south by the Antarctic continent but, open to the north and east for interaction with waters of the ACC. CDW is advected into the eastern side of the gyre and can be identified by maxima in temperature, salinity and nutrients within the gyre (Deacon, 1979; Whitworth and Nowlin, 1987; Gouretski and Danilov, 1993; Schroder and Fahrbach, 1999). A substantial part of the ocean is ventilated in the Weddell Gyre as a result of the formation of deep and bottom waters due to strong atmosphere–ice–ocean interactions (Gill, 1973; Carmack and Foster, 1975). Early studies largely regarded this region as a source of CO_2 due to the upwelling of the CO_2-rich deep water (Deacon, 1979; Weiss et al., 1979; Takahashi et al., 1993). Since then, several investigations into the carbonate chemistry of the Weddell Gyre have shown this area to be a net sink for atmospheric CO_2 (Hoppema et al., 1995; Hoppema et al., 1999; Stoll et al., 1999; Hoppema et al., 2000; Stoll et al., 2002; Bakker et al., 2008).

In the western Atlantic sector of the Southern Ocean, the SB lies just north of the Weddell–Scotia Confluence, which extends from the Antarctic Peninsula to about 20°W (Patterson and

*Corresponding author.
e-mail: elizabeth.jones@uea.ac.uk
DOI: 10.1111/j.1600-0889.2010.00496.x

Sievers, 1980; Whitworth et al., 1994), separating the Weddell Sea to the south from the ACC in the Scotia Sea to the north (Orsi et al., 1995). The Weddell–Scotia Confluence provides a transition zone where the recently ventilated waters flow out of the Weddell Sea and into the Scotia Sea (Patterson and Sievers, 1980; Orsi et al., 1999; Naveira Garabato et al., 2002). Therefore, it is important to improve the understanding of the ocean carbonate chemistry of the Weddell–Scotia Confluence and its contribution to the Southern Ocean carbon cycle.

Increased biomass and productivity are regularly observed in MIZs (Smith and Nelson, 1986; Kang et al., 2001; Korb et al., 2005) due to factors including water-column stability (Smith and Nelson, 1985; Holm-Hansen and Mitchell, 1991; Sakshaug et al., 1991; Lancelot et al., 1993), seeding by ice algae (Smith and Nelson, 1985; Ackley and Sullivan, 1994) and the release of bioavailable iron (de Baar et al., 1990; Martin, 1990; Sedwick and DiTullio, 1997). Additional supplies of iron into surface waters of the Weddell–Scotia Confluence could originate from upwelling within the ACC (Hoppema et al., 2003; Blain et al., 2007) and advection from waters flowing out from the tip of the Antarctic Peninsula (Nolting et al., 1991; Sanudo-Wilhelmy et al., 2002; Dulaiova et al., 2009). These processes have been implicated in the enhanced productivity and ecological diversity associated with the Weddell–Scotia Confluence (Jacques and Panouse, 1991; Comiso et al., 1993; Helbling et al., 1993; Tynan, 1998; Holm-Hansen and Hewes, 2004; Hewes et al., 2008).

Field and laboratory studies have shown that ikaite, a hydrous calcium carbonate mineral ($CaCO_3{\cdot}6H_2O$), precipitates out within brines during sea ice formation (Marion, 2001; Papadimitriou et al., 2004; Delille et al., 2007; Papadimitriou et al., 2007; Rysgaard et al., 2007; Dieckmann et al., 2008):

$$Ca^{2+}(aq) + 2HCO_3^-(aq) + 5H_2O(l) \leftrightarrow CaCO_3 \cdot 6H_2O(s) + CO_2(aq). \quad (1)$$

The net effect of ikaite precipitation in brine is to reduce the concentration of dissolved inorganic carbon (DIC) and total alkalinity (TA), whilst increasing the fugacity of CO_2 (fCO_2, eq. 1). Any brine rejected during winter or released during ice melt transfers these inorganic carbon characteristics to the underlying water. One implication of these processes is that during sea ice growth, the winter mixed layer becomes isolated from the atmosphere (Klatt et al., 2002), allowing levels of fCO_2 to reach supersaturation beneath the sea ice. During sea ice melt in spring and summer, any remaining carbonate minerals within the ice are thought to be released into the water column where they re-enter the carbon cycle through dissolution. According to eq. (1), this would increase TA and DIC and reduce fCO_2 of the water.

The activity of ice algae also leads to changes in the carbonate system of the brine and the water at the ice–sea interface (Gleitz et al., 1995; Gleitz et al., 1996; Gibson and Trull, 1999; Krembs and Engel, 2001; Meiners et al., 2009). During summer, increased light levels promote photosynthesis, reducing DIC and the fCO_2 of the brine. As the ice melts, these carbonate characteristics are transferred to the surrounding water, becoming superimposed on effects from carbonate mineral chemistry.

The sea ice carbonate chemistry processes have been described as a 'sea ice CO_2 pump', assuming dissolution of ikaite in the summer promotes atmospheric CO_2 uptake and that DIC- and TA-poor, but CO_2-rich brines are transported out of the surface waters during the winter (Rysgaard et al., 2007). The MIZs of the Southern Ocean are of great interest due to the effects of enhanced biological activity and, more recently, calcium carbonate chemistry on the oceanic carbon cycle. However, few data exist to investigate and quantify the carbonate chemistry processes in melting polar sea ice and to infer the implications of the sea ice carbon pump for the global carbon cycle. In this paper, we present direct measurements of fCO_2, DIC and TA from waters at and around the receding ice edge. The distribution of upper ocean carbonate chemistry in the Weddell–Scotia Confluence during austral summer is evaluated within the context of physical and biological controls, including (1) the influence of sea ice cover; (2) the effect of recent sea ice melt and an ice edge bloom and (3) the influence of the SB.

2. Methods

2.1. Underway and station sampling

Data were collected in the Weddell–Scotia Confluence during cruise JR177 on the RRS *James Clark Ross* in January 2008 (Fig. 1). The ship reached the South Orkney Islands on 8 January 2008 and made two transects in the Weddell–Scotia Confluence, southward and northward, passing the ice edge overlying the South Orkney shelf at station 5 (Table 1, Fig. 2). The southward transect ended in the sea ice at station 1 (62.61°S 43.24°W), over the break of the South Orkney shelf on 11 January. Between stations 1 and 6 the ship sailed through waters with partial sea ice cover, melting sea ice and areas of open water. The ship left the MIZ on 13 January and continued northward to the SB at station 13 (59.14°S 43.69°W) on 17 January.

Continuous measurements of temperature and salinity in surface water were made using seawater from the non-toxic underway supply (bow intake 6.5 m below the surface). High resolution, vertical profiles of potential temperature and salinity were obtained during the downcast using a conductivity, temperature and depth (CTD) sensor (Seabird SBE9+). An offset in sea surface temperature (0.37 °C) was detected between the ship's oceanlogger temperature sensor and the CTD surface temperature, which has been applied to the underway temperature dataset. All salinity values are reported on the practical salinity scale.

The summer mixed layer depth (MLD) is defined here as the depth where the potential density exceeds that measured at 10 m by 0.05 kg m^{-3} (Brainerd and Gregg, 1995). This definition

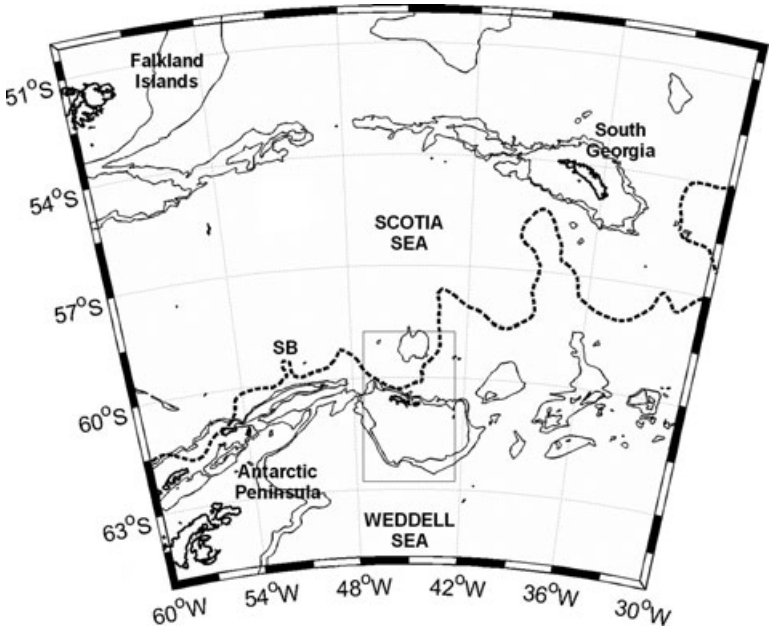

Fig. 1. Map of the Weddell–Scotia Confluence region. The boxed area shows the research site, see Fig. 2 for further details. The dashed line represents the Southern Boundary (SB) at the time of sampling with the dynamic height for the front selected after comparison with the hydrographic section. The absolute dynamic height topography data were produced by Ssalto/Duacs and distributed by Aviso (http://www.aviso.oceanobs.com) with support from the Centre National d'Etudes Spatiales (CNES). Depth contours are at 1000 and 2000 m (GEBCO, 2001).

Table 1. Station number, classification, date, location (°S, °W) and bottom depth (m) for all hydrographic stations in the Weddell–Scotia Confluence

Station	Classification	Date	Latitude (°S)	Longitude (°W)	Bottom depth (m)
9	Open water	8 Jan 2008	60.208	44.408	5543
8	Open water	9 Jan 2008	60.431	44.593	999
6	Meltwater	10 Jan 2008	61.198	44.408	319
5	Ice edge	10 Jan 2008	61.665	44.053	570
3	Sea ice	11 Jan 2008	62.355	43.529	1238
1	Sea ice	11 Jan 2008	62.608	43.234	3075
10	Open water	13 Jan 2008	59.936	44.239	4784
11	Open water	15 Jan 2008	59.689	44.054	4172
13	Southern Boundary	17 Jan 2008	59.144	43.694	3611

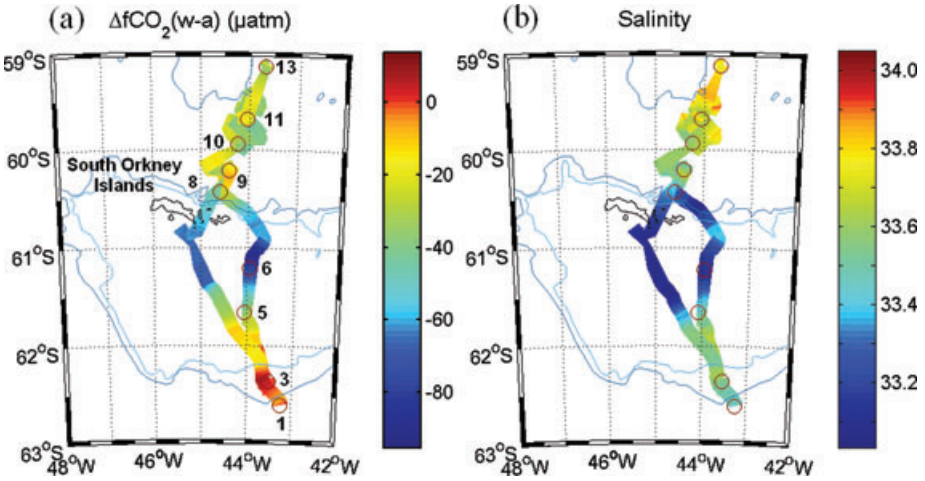

Fig. 2. The research area showing (a) ΔfCO_2 (water–air) (μatm) and (b) sea surface salinity along the two transects and the station locations. The marginal ice zone (MIZ), south of the South Orkney Islands, includes stations 1, 3, 5 and 6. Depth contours are at 1000 and 2000 m (GEBCO, 2001).

was selected to provide a depth that is located between the active mixing layer and the seasonal mixed layer. MLDs were calculated from 2 dbar profiles of the potential temperature and salinity from the CTD deployment at each station. The winter mixed layer, marking the remnant of the Winter Water (WW), is defined here as the depth of the potential temperature minimum ($\theta_{\min}$) (Brainerd and Gregg, 1995). For all stations, the WW layer was identified by a well-defined $\theta_{\min}$ at depths in the range of 60–100 m.

2.2. *Fugacity of CO_2 in surface seawater and the atmosphere*

Quasi-continuous measurements of the fCO_2 in surface water were made using an underway fCO_2 system and seawater from the underway supply (Schuster and Watson, 2007). Atmospheric samples were taken from an air inlet located forward at 15 m height on the ship's bridge. Mixing ratios of CO_2 and moisture in the equilibrator headspace and the outside air were determined by circulation through a non-dispersive infrared analyser (Li-COR 7000). The Li-COR was calibrated using three secondary gas standards of known CO_2 concentrations of 249.1 $\pm$ 0.2, 356.5 $\pm$ 0.2 and 457.4 $\pm$ 0.2 μmol mol^{-1} in an air mixture (21% O_2, 79% N_2). All gases underwent pre- and post-cruise calibration against certified, high precision, primary standards from the National Oceanic and Atmospheric Administration (NOAA). Samples from the equilibrator headspace and marine air were partially dried by being passing through an electric cool box at about 2 °C, prior to analysis in the Li-COR. The fCO_2 for equilibrated water samples and the air was computed from the partly dried mixing ratios and ambient barometric pressure and then corrected for seawater vapour pressure (assuming saturation at the sea surface).

Two platinum resistant thermometers positioned in the upper and lower part of the seawater stream determined the temperature of the water in the equilibrator. Warming of the seawater between the intake and the equilibrator was on average 0.8 °C (σ = 0.1 °C; n = 250). Sea surface fCO_2 data were corrected to sea surface temperature to account for this warming (Takahashi et al., 1993). The difference in fCO_2 between the seawater and overlying air [$\Delta fCO_2(w-a)$] was calculated continuously during the cruise. The time lag between sampling and the seawater reaching the equilibrator was 116 seconds, which has been corrected for. Sea surface fCO_2 from the underway supply was co-located to the CTD casts by interpolation to the time of the 5 m sample from the upcast of the CTD. Gaps in the data are due to the seawater supply being turned off in thick ice cover or contamination from the ship exhaust gases. The accuracy of the marine air fCO_2 data was determined as 0.6 μatm from comparisons with atmospheric data from Jubany Station, South Shetland Islands (62.23°S 58.67°W) (Ciattaglia et al., 1999). The precision of the fCO_2 data is 3.0 μatm.

2.3. *Carbonate system*

Underway samples for sea surface DIC and TA analysis were collected from the underway seawater supply. Vertical profile samples were taken from the 24 $\times$ 10 L Niskin bottles mounted onto the CTD rosette at 5, 10, 30, 50, 80, 120, 160 and 200 m depth on the upcast of the CTD. Seawater (250 or 500 ml) was collected in borosilicate glass bottles and a small volume was extracted to create a head space. Saturated aqueous mercuric chloride was immediately added (0.02% vol/vol) and the bottle was sealed, shaken and stored in a dark location at ambient temperature for shipment to the UK.

The DIC concentration was determined by coulometric analysis (Johnson et al., 1987) and TA analyses were carried out by potentiometric titration with hydrochloric acid (Dickson, 1981) using a VINDTA instrument from April to May 2008. Duplicate analyses were made for each 500 ml bottle. Two bottles of certified reference material (CRM) from batches 76 or 81 (DOE, 2007) were analysed in duplicate per CTD cast and per 10 samples from the underway supply. DIC and TA values were corrected to account for the dilution of the seawater by the addition of mercuric chloride solution. The accuracy for the DIC and alkalinity measurements is determined as 2 μmol kg^{-1} (n = 96) from the average difference between certified and calculated values for each CRM analysis. The precision for the DIC and alkalinity measurements is estimated as better than 2 μmol kg^{-1} (n = 96) based on the average difference between duplicate CRM bottle analyses. DIC and TA from all sea surface samples were used to calculate fCO_2, f(DIC,TA), using the CO2Sys programme (Lewis and Wallace, 1998) with thermodynamic dissociation constants for K_1 and K_2 by Mehrbach et al. (1973) and the re-fit by Dickson and Millero (1987).

All surface alkalinity samples showed strong salinity dependence with a positive intercept of 269 μmol kg^{-1} (TA_0) at zero salinity. To correct for dilution or concentration effects, TA data were normalized to salinity 34.3, the average salinity of the WW for all stations in the Weddell–Scotia Confluence, using eq. (2) to account for the non-zero end-member (Friis et al., 2003)

$$TA_{34.3} = \left(\frac{TA - TA_0}{S}\right) 34.3 + TA_0. \quad (2)$$

This was repeated for the DIC data, where a value of 966 μmol kg^{-1} was determined for DIC_0. A series of de-ionized water samples were analysed to determine a 'blank' for DIC and TA at zero salinity. Average values for $TA_{0\_de\text{-}ionzed}$ and $DIC_{0\_de\text{-}ionzed}$ of 74 $\pm$ 11 and 36 $\pm$ 3 μmol kg^{-1} (n = 6), respectively, indicate that the TA_0 and DIC_0 determined for the Weddell–Scotia Confluence samples do not result from the analytical technique but from natural sources, which could include dissolution of carbonate minerals during the analysis and bacterial degradation. DIC and TA measurements reported in the text are not salinity normalized unless stated.

2.4. Macronutrients

Underway samples from the underway seawater supply and CTD water bottle samples were filtered through a mixed ester membrane (Whatman, pore size 0.45 μm), and the filtrate was analysed colorimetrically for dissolved silicate (SiO_4^{4-}), phosphate (PO_4^{3-}) and nitrate (NO_3^-) with a segmented-flow analyser (Technicon, Whitehouse, 1997). Analyses for nitrate included nitrite (NO_2), which is not considered separately as its concentration had little variation and was typically <1% of total $NO_3 + NO_2$. Nutrient data were normalized to salinity 34.3 using a direct normalization procedure by multiplication with 34.3 and division by the in situ salinity. Nutrient concentrations reported in the text are not salinity normalized unless stated.

2.5. Chlorophyll-a

Underway samples for sea surface chlorophyll-a were collected from the non-toxic seawater supply approximately every hour as the ship was in transit. Water samples were filtered through glass fibre filters (Whatman GF/F) under low (<70 mm Hg) vacuum pressure and immediately frozen and stored at −20 °C until analysis onboard. The samples on the filters were then extracted in acetone (10 ml, 90%) in the dark for 24 h (Parsons et al., 1984). Fluorescence of the extract was measured before and after acidification with 1.2 M HCl on a TD-700 Turner fluorometer. The instrument was calibrated against commercially prepared chlorophyll-a standards (Sigma).

2.6. Sea ice

Visual observations of sea ice coverage were made from the vessel's bridge as part of the daily position report filed by the Captain. The observations included primary ice types present, the sea ice coverage and meteorological conditions. Daily sea ice concentration data at 4 km resolution were obtained through the Operational SST and Sea Ice Analysis (OSTIA) service, a component of the Group for High-Resolution Sea Surface Temperature (GHRSST) at http://ghrsst-pp.metoffice.com/pages/latest_analysis/ostia.html (Stark et al., 2007). The transition area between open ice-free waters to ice-covered waters is referred to as the MIZ, encompassing stations 1, 3, 5 and 6 during the present study. The ice edge is defined here as the position where consolidated sea ice was first encountered (station 5) on the southern transect.

2.7. Seasonal biogeochemical deficits

The seasonal depletion in DIC, alkalinity and nutrients was determined for each station from the difference between the average concentration in the summer mixed layer and the concentration at the depth of the θ_{min}, in the WW (Jennings et al., 1984). The biogeochemical properties of the WW have previously been used as proxies for conditions present in Southern Ocean surface waters during the preceding winter (e.g. Minas and Minas, 1992; Ishii et al., 1998; Rubin et al., 1998; Pondaven et al., 2000; Ishii et al., 2002). The validity of this method for the Weddell–Scotia Confluence data is discussed below. For the sea ice stations (1–6), values for the θ_{min} were between −1.60 and −1.70 °C (Table 2). Satellite derived sea ice cover indicated that the break-up of the sea ice (last day when ice cover was ≥90%) occurred in early December, 4 weeks prior to sampling. Therefore, top-down warming was very recent and any erosion of the winter mixed layer was attributed to vertical mixing of warmer waters below the thermocline. To estimate any bottom-up influences, the value of the θ_{min} was compared to the temperature at the base of the thermocline, assuming an end member winter mixed layer temperature of −1.70 °C and that the specific heat capacity of seawater was constant. For the range of θ_{min} values, mixing from deeper waters from winter to summer is estimated at 4–7%. This could lead to a slight over estimation in winter DIC and TA as highlighted during a comparable seasonal

Table 2. Winter mixed layer depth (WMLD, m), temperature (°C), salinity, silicate (SiO_4, μmol kg^{-1}), phosphate (PO_4, μmol kg^{-1}), nitrate (NO_3, μmol kg^{-1}), dissolved inorganic carbon (DIC, μmol kg^{-1}) and total alkalinity (TA, μmol kg^{-1}) of the winter mixed layer (representing the WW) for all stations in the Weddell–Scotia Confluence from 62.61°S (station 1) to 59.14°S (station 13)

Station	WMLD (m)	θ_{min} (°C)	Salinity	SiO_4 (μmol kg^{-1})	PO_4 (μmol kg^{-1})	NO_3 (μmol kg^{-1})	DIC (μmol kg^{-1})	TA (μmol kg^{-1})
1	61	−1.65	34.33	82.8	1.96	28.3	2224	2328
3	57	−1.60	34.28	84.6	1.97	29.6	2224	2332
5	69	−1.70	34.24	80.3	1.94	31.0	2222	2325
6	67	−1.63	34.14	78.0	1.81	29.5	2214	2325
8	71	−1.56	34.24	84.4	1.93	29.0	2218	2326
9	87	−1.56	34.20	80.8	1.94	28.8	2213	2326
10	91	−1.46	34.30	84.4	2.02	28.8	2220	2333
11	97	−1.35	34.30	83.5	2.02	31.2	2223	2332
13	93	−1.39	34.25	83.2	1.99	31.6	2222	2330

Notes: The absolute value for each station is shown measured from 1 bottle at the depth of the potential temperature minimum (θ_{min}). Stations 6 and 13 have interpolated nutrient concentrations from proximal stations 8 and 11, respectively.

study in the Indian sector of the Southern Ocean (Jouandet et al., 2008).

The total DIC deficit ($\Delta DIC_{deficit}$) can be expressed as a sum of contributing processes, represented by the following:

$$\Delta DIC_{deficit} = \Delta DIC_{salinity} + \Delta DICC_{org} + \Delta DICCaCO_3 + \Delta DIC_{residual}. \quad (3)$$

Deficits in DIC due to salinity changes are determined from the difference between the measured and salinity normalized DIC deficit. A composite error of 2 μmol kg^{-1} is associated with the $\Delta DIC_{salinity}$ term. Modifications in DIC due to abundance of organic matter through photosynthesis and respiration (ΔDIC_{Corg}) have been estimated from normalized nitrate deficits (Sweeney et al., 2000), assuming a carbon to nitrogen uptake ratio of 117:16 moles (Anderson and Sarmiento, 1994). Comparisons to phosphate utilization by Redfield stoichiometry (Redfield et al., 1963) indicate uncertainties in ΔDIC_{Corg} of 1–9 μmol kg^{-1}. The deficit in alkalinity, corrected for salinity and organic matter effects, indicates carbonate mineral (ikaite) precipitation or dissolution based on 2:1 changes in TA and DIC (Zeebe and Wolf-Gladrow, 2001). A composite error of 3 μmol kg^{-1} accompanies the carbonate term. The residual term accounts for the remaining seasonal deficit as a result of processes including CO_2 air–sea exchange, surface advection and slight vertical mixing (see above). The associated error is the sum of that for each term in eq. (3).

3. Results

3.1. Hydrography

Surface waters (0–20 dbar) showed a strong northward gradient in potential temperature from about −1.4 °C beneath the sea ice to greater than 1.0 °C at about 59°S (Fig. 3b). Surface salinity showed a similar trend, increasing from values close to 33.5 beneath the sea ice to values above 33.8 at 59°S (Fig. 3a). A notable exception to this trend was the distinct reduction in salinity in the region of substantial sea ice melt to the south of the South Orkney Islands, at and around station 6 (Table 3, Fig. 2b).

A distinct WW layer could be observed for all stations, with an average potential temperature minimum (θ_{min}) of −1.55 ± 0.12 °C and a winter MLD of 79 ± 15 m (n = 9, Table 2). Potential temperature of the WW predominantly followed the increasing northward trend of summer mixed layer potential temperature. In comparison, WW salinity was much more variable, from the most saline WW beneath the sea ice decreasing to the freshest water in the region of substantial ice melt. North of the MIZ, WW salinity increased from values close to 34.2 over the South Orkney shelf up to about 34.3 at 59°S.

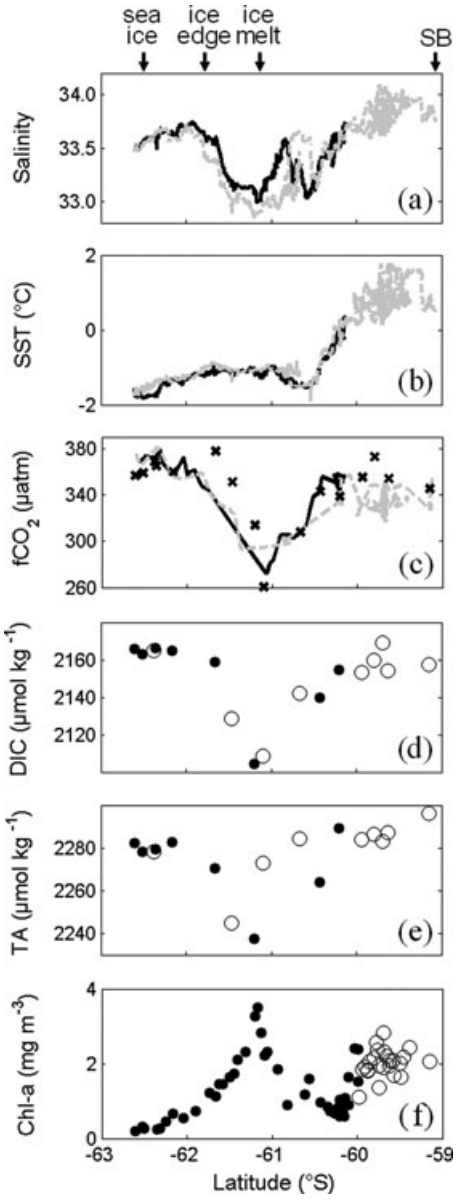

Fig. 3. The latitudinal distribution of sea surface (a) salinity, (b) temperature (SST, °C), (c) $fCO_{2measured}$ (lines, μatm) and $fCO_{2calculated}$ (crosses, μatm), (d) dissolved inorganic carbon (DIC, μmol kg^{-1}), (e) total alkalinity (TA, μmol kg^{-1}) and (f) chlorophyll-a (chl-a, mg m^{-3}) for the southward (solid line, filled circles) and northward (dashed line, open circles) transects across the Weddell–Scotia Confluence. The data show values for station and underway samples.

3.2. Macronutrients

Surface silicate (hereinafter SiO_4) concentrations were generally high (≥70 μmol kg^{-1}) throughout the Weddell–Scotia Confluence (Table 3). The SiO_4 concentration showed a slight decreasing gradient for stations 1–6 in the MIZ and a more homogenous distribution north of the MIZ (stations 8–13). Surface nitrate (hereinafter NO_3) and phosphate (hereinafter

Table 3. Mixed layer depth (MLD, m), temperature (°C), salinity, silicate (SiO_4, μmol kg^{-1}), phosphate (PO_4, μmol kg^{-1}) and nitrate (NO_3, μmol kg^{-1}) of the summer mixed layer for all stations in the Weddell–Scotia Confluence from 62.61°S (station 1) to 59.14°S (station 13)

Station	*n*	MLD (m)	Temperature (°C)	Salinity	SiO_4 (μmol kg^{-1})	PO_4 (μmol kg^{-1})	NO_3 (μmol kg^{-1})
1	2	23	−1.40 (0.02)	33.54 (0.02)	80.5 (0.2)	1.82 (0.00)	27.1 (0.2)
3	2	25	−1.41 (0.00)	33.60 (0.00)	71.7 (0.2)	1.73 (0.01)	26.4 (0.1)
5	2	19	−0.76 (0.00)	33.57 (0.00)	69.5 (0.1)	1.62 (0.00)	25.6 (0.2)
6	2	17	−0.65 (0.02)	33.23 (0.23)	66.0 (0.1)	1.42 (0.01)	23.4 (0.2)
8	2	23	−0.63 (0.01)	33.35 (0.00)	73.4 (0.3)	1.58 (0.01)	24.4 (0.5)
9	3	29	−0.01 (0.11)	33.64 (0.01)	74.3 (0.2)	1.60 (0.01)	24.1 (0.2)
10	3	33	0.64 (0.06)	33.70 (0.02)	74.9 (0.1)	1.44 (0.03)	23.2 (0.1)
11	2	17	0.94 (0.01)	33.71 (0.00)	73.0 (0.2)	1.48 (0.02)	22.8 (0.2)
13	2	29	1.09 (0.01)	33.85 (0.00)	71.0 (0.3)	1.34 (0.01)	22.4 (0.0)

Notes: The mean value for each station is shown (from values measured at *n* bottle depths up to the MLD) with the standard deviation (for stations where $n > 2$) and the difference (for stations where $n = 2$) in brackets. Stations 6 and 13 have interpolated nutrient concentrations from proximal stations 8 and 11, respectively.

PO_4) concentrations showed general decreasing northward trends with average values of 24.3 and 1.56 μmol kg^{-1}, respectively. Compared to sea ice stations 1, 3 and 5, large depletion of all three macronutrients had occurred in the region of extensive ice melt at station 6. Average WW concentrations for SiO_4, NO_3 and PO_4 were 82.4, 30.1 and 1.95 μmol kg^{-1}, respectively, with lower values at station 6 (Table 2). Concentrations of NO_3 and PO_4 are similar to WW values measured further north in the Scotia Sea and higher concentrations of SiO_4 are consistent with the major gradient that exists for this macronutrient in this region (Whitehouse et al., 2008).

3.3. Chlorophyll-a and phytoplankton species distribution

Chlorophyll-a concentrations ([chl-a]) varied between 1.85 and 2.84 mg m^{-3} (Fig. 3f) in the open waters of the Weddell–Scotia Confluence, south of 59°S to about 60°S (stations 10–13). A summer maximum in chlorophyll-a of 3.51 mg m^{-3} was observed in the melt waters at and around station 6, signifying the presence of a phytoplankton bloom (defined here as [chl-a] $\geq$ 2.0 mg m^{-3}). Chlorophyll-a concentrations sharply decreased to a minimum of 0.21 mg m^{-3} beneath the sea ice at station 1. For the MIZ (stations 1–6), the phytoplankton community was dominated by naked, heterotrophic dinoflagellates with diatoms accounting for between 21 and 46% of the total cell abundance (Korb et al., 2010). North of the South Orkney Islands to 59°S (stations 8–13) the community consisted of a mixture of dinoflagellates and cryptophytes, with less than 20% diatoms (Korb et al., 2010).

3.4. Carbonate chemistry

Contrasting concentrations of fCO_2, DIC and TA were observed in and around the sea ice edge and within the frontal waters of the SB (Figs 3c–e). The fCO_2 varied from supersaturation with ΔfCO_2 of 14 μatm in waters beneath the sea ice to strong undersaturation with ΔfCO_2 of −95 μatm in the region of substantial ice melt (Fig. 2). Calculated fCO_2 [f(DIC,TA)] generally showed a close agreement to measured fCO_2, apart from a positive offset due to higher calculated fCO_2 values from the ice edge to the meltwater region (Fig. 3c).

The concentration of sea surface DIC showed similar patterns and predominantly followed the trend of the fCO_2 observations (Fig. 3d). The highest concentration of DIC, TA and the highest value of fCO_2 were measured beneath the sea ice close to station 1 (Table 4). Relative to all other MIZ stations, DIC, TA and fCO_2 reached distinct summer minima in the region of extensive ice melt (Fig. 3). Sea surface normalized DIC ($DIC_{34.3}$) predominantly followed the trend in DIC concentrations, decreasing from values greater than 2190 μmol kg^{-1} beneath the sea ice to values around 2180 μmol kg^{-1} at the SB (Table 4). An exception to this gradual decreasing trend was at station 6, where a substantial reduction in $DIC_{34.3}$ of up to 40 μmol kg^{-1} was observed, relative to the average $DIC_{34.3}$ in the summer mixed layer at all other stations. Sea surface normalized TA ($TA_{34.3}$) showed a similar variation, with the highest values of about 2332 μmol kg^{-1} in the area of greater sea ice coverage and the lowest values in the region of extensive sea ice melt (stations 5 and 6).

Across the Weddell–Scotia Confluence, WW DIC and $DIC_{34.3}$ were relatively homogenous with average concentrations of about 2220 μmol kg^{-1} (Table 2). Alkalinity showed more variation, with distinct low values at MIZ stations in and near the area of greatest sea ice melt. There was an overall northward increase in $TA_{34.3}$ of the WW.

4. Discussion

4.1. Sea surface carbonate chemistry during summer ice melt

The processes affecting carbonate chemistry in waters at and around the ice edge will be investigated by comparing surface

Table 4. Dissolved inorganic carbon (DIC, μmol kg^{-1}), total alkalinity (TA, μmol kg^{-1}), salinity normalized DIC (DIC$_{34.4}$, μmol kg^{-1}) and salinity normalized TA (TA$_{34.3}$, μmol kg^{-1}) of the summer mixed layer and surface water $fCO_{2measured}$ (μatm), $fCO_{2calculated}$ [as f(DIC,TA), μatm] and chlorophyll-a (chl-a, mg m^{-3}) for all stations in the Weddell–Scotia Confluence from 62.61°S (station 1) to 59.14°S (station 13)

Station	n	DIC (μmol kg^{-1})	TA (μmol kg^{-1})	DIC$_{34.3}$ (μmol kg^{-1})	TA$_{34.3}$ (μmol kg^{-1})	$fCO_{2measured}$ (μatm)	$fCO_{2calculated}$ (μatm)	Chl-a (mg m^{-3})
1	2	2169 (7)	2286 (7)	2196 (6)	2332 (7)	377	357	0.21
3	2	2166 (1)	2280 (2)	2191 (1)	2322 (2)	375	359	0.24
5	2	2159 (1)	2273 (5)	2185 (1)	2316 (5)	336	378	1.14
6	2	2105 (2)	2252 (28)	2142 (7)	2315 (15)	294	314	3.51
8	2	2140 (0)	2265 (1)	2173 (0)	2321 (1)	345	343	0.96
9	3	2156 (3)	2289 (2)	2180 (3)	2328 (2)	352	339	0.60
10	3	2152 (7)	2293 (8)	2174 (7)	2329 (8)	340	355	1.85
11	2	2169 (1)	2290 (14)	2190 (1)	2325 (14)	334	406	2.84
13	2	2161 (8)	2299 (4)	2177 (8)	2326 (4)	332	346	2.06

Note: The mean value for DIC, DIC$_{34.3}$, TA and TA$_{34.3}$ is shown (from values measured at n bottle depths up to the depth of the mixed layer) with the standard deviation (for stations where $n > 2$) and the difference (for stations where $n = 2$) in brackets.

water fCO_2, DIC and TA measured at the contrasting sites in the MIZ. To the south of the South Orkney Islands (stations 1–3), the sea surface was characterized by large plates of consolidated sea ice as well as regions where the ice pack had begun to break up. Macronutrient concentrations were the highest (Table 3) and chlorophyll-a reached the lowest concentration of 0.21 mg m^{-3} (Table 4) for whole Weddell–Scotia Confluence. Surface temperatures in excess of the freezing point of seawater and reduced salinity, compared to station 5 at the ice edge, indicate that slight sea ice melt had occurred (Fig. 4). Effects of sea ice melt were most pronounced at station 6 (Fig. 2b), where the site was largely open water with sporadic ice floes. Substantial sea ice melt had stabilized the upper water column by forming a warm and shallow meltwater lens at the surface (Fig. 4), which supported elevated chlorophyll-a (Fig. 3f). This corresponded to a rapid reduction in sea surface DIC by 53 μmol kg^{-1} and fCO_2 by 55 μatm, compared to all other stations, driving a strong CO_2 undersaturation of 74 μatm at station 6 (Fig. 2a).

Melting sea ice forms shallow mixed layers with favourable light conditions that promote the development of phytoplankton blooms in the meltwaters (Smith and Nelson, 1986; Lancelot et al., 1993). Blooms associated with the receding ice edge have been previously observed in the MIZ of the Weddell–Scotia Confluence region (Buma et al., 1992; Lancelot et al., 1993; Kang et al., 2001; Korb et al., 2005). The bloom in the meltwaters at station 6 could be partially sustained by natural iron enrichment from melting sea ice (Löscher et al., 1997; Lannuzel et al., 2007; Lannuzel et al., 2008), vertical mixing over shallow topography (Table 1), upwelling in the ACC (Hoppema et al., 2003; Blain et al., 2007) or advection from the Antarctic Peninsula region (Nolting et al., 1991; Sanudo-Wilhelmy et al., 2002; Dulaiova et al., 2009). Recent evidence strongly suggests that iron is advected into the Scotia Sea from the South Shetland Islands and the Antarctic Peninsula, supporting phytoplankton growth in this downstream region (Ardelan et al., 2010). It has been inferred that it is the interaction between iron and light that limits the initiation and maintenance of blooms in the MIZ (Korb et al., 2005, and references cited therein).

In addition, diatoms in sea ice can act as an inoculum and seed the formation of phytoplankton blooms when released upon sea ice melt (Smith and Nelson, 1985; Ackley and Sullivan, 1994). Diatom activity reduces the concentrations of macronutrients and DIC in the sea ice brine. These chemical signatures are transferred to the surrounding water as the sea ice melts. It is likely that a combination of these processes stimulated the formation and growth of the bloom in the meltwaters of the Weddell–Scotia Confluence and contributed to the reductions in DIC and macronutrient concentrations within the shallow mixed layer (Figs 3 and 4).

Changes in concentrations of macronutrients were compared to DIC$_{34.3}$ to investigate whether biological utilization of nutrients had occurred (Figs 5a–c). Nitrate and phosphate showed similar decreasing concentrations with decreasing DIC$_{34.3}$, which suggests nutrient depletion as a result of phytoplankton growth. The ratio of the change in DIC$_{34.3}$ with respect to nitrate (7) is very similar to that determined from phytoplankton decomposition analyses, C:N:P of 106:16:1 (Redfield et al., 1963), and to that calculated by examination of spatial changes in nutrient concentrations, C:N:P of 117:16:1 (Anderson and Sarmiento, 1994). The gradient of the phosphate regression line (48) is much smaller than that predicted by either nutrient utilization ratio. The decreasing concentration of silicate indicates the activity of the diatoms observed in this region (Korb et al., 2010). Despite the bloom being dominated by naked dinoflagellates, with little photosynthetic ability, it is predicted that the few diatoms present would account for the majority of the photosynthetic activity and carbon utilization. Based on the DIC$_{34.3}$, TA$_{34.3}$ and nutrient deficits, photosynthesis had reduced nutrients and DIC by approximate Redfield ratios. Deviations from predicted nutrient depletion ratios may be due other processes,

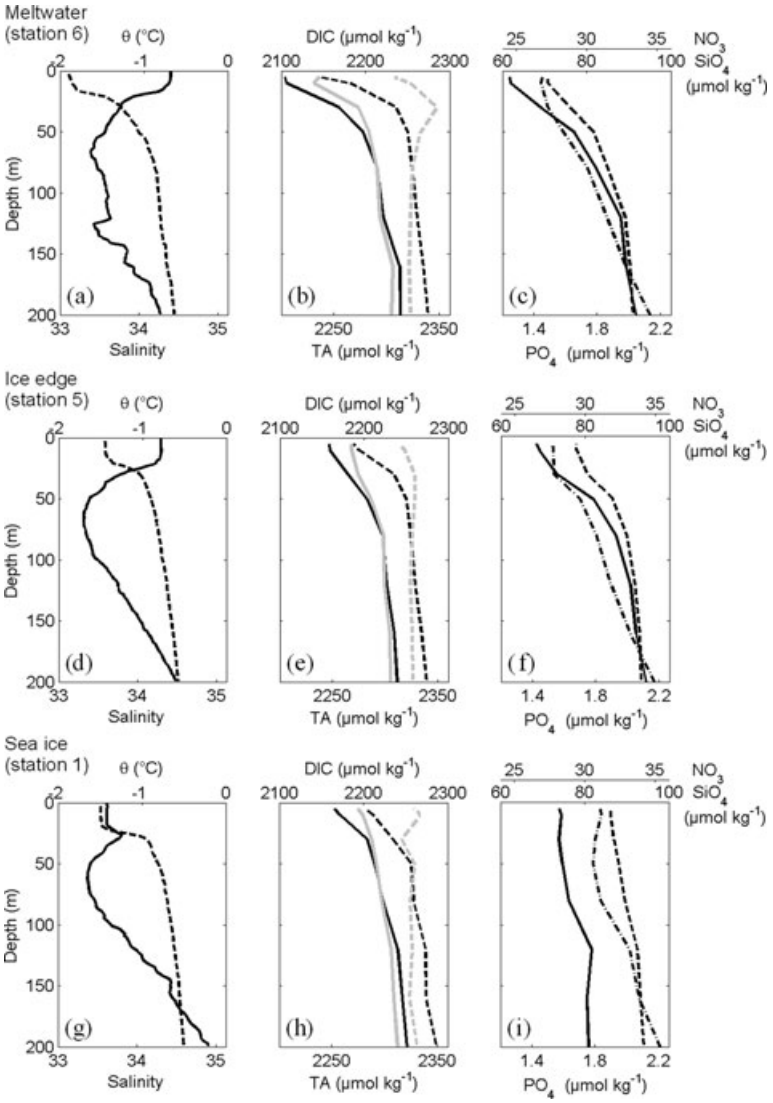

Fig. 4. Vertical profiles of upper water column (a, d, g) potential temperature (θ, solid line, °C) and salinity (dashed line), (b, e, h) dissolved inorganic carbon (DIC, black solid line, μmol kg^{-1}), total alkalinity (TA, black dashed line, μmol kg^{-1}), salinity normalized DIC (grey solid line, μmol kg^{-1}), salinity normalized TA (grey dashed line, μmol kg^{-1}) and (c, f, i) nitrate (NO_3, solid line, μmol kg^{-1}), phosphate (PO_4, dashed line, μmol kg^{-1}) and silicate (SiO_4, dot–dashed line, μmol kg^{-1}), in meltwaters (station 6), at the ice edge (station 5) and beneath the sea ice (station 1).

including sea ice carbonate chemistry, which will now be investigated.

A relationship between $DIC_{34.3}$ and $TA_{34.3}$ of 1:2 is indicative of ikaite ($CaCO_3 \cdot 6H_2O$) precipitation, following eq. (1). Changes in $DIC_{34.3}$ and $TA_{34.3}$ for the MIZ stations (1–6) group together in a decreasing trend close to 1:2, with the exception of station 6 (Fig. 5d). During sea ice formation and growth, precipitation of ikaite creates DIC- and TA-poor and fCO_2-rich brines. Any brine remaining in channels and pockets within the sea ice matrix is released into the underlying water during sea ice melt, which would have the net effect of reducing $TA_{34.3}$ and $DIC_{34.3}$ (2:1) at the surface. Using salinity as a proxy for ice melt (Fig. 2b), in conjunction with in situ and satellite observations, sea ice melt was evident to some degree at all stations in the MIZ during summer 2008. We put forward the hypothesis that ikaite precipitation had occurred in the sea ice brines of the Weddell–Scotia Confluence during the preceding winter and the resultant DIC- and TA-poor brines were released into the underlying water as the ice melted, transferring the inorganic carbon characteristics into the summer mixed layer. The absence of calcifying phytoplankton in this region (Korb et al., 2010) supports the proposed mechanism of the observed depletion in DIC and TA at the sea surface.

An outlier to the principle trend is station 6 in the meltwaters supporting a phytoplankton bloom. Although not numerically dominant within the bloom, diatoms had rapidly reduced $DIC_{34.3}$ by 35 μmol kg^{-1} at the sea surface, compared to ice edge station 5. Based on the $DIC_{34.3}$ and nutrient distributions for the MIZ stations (Fig. 5), biological carbon uptake had further reduced the DIC signature from the released brine, driving a strong undersaturation in fCO_2 at the sea surface.

A notable feature in sea surface fCO_2 was the higher calculated fCO_2 values along the strong fCO_2 gradient that existed from the ice edge to the meltwater region (Fig. 3c). This

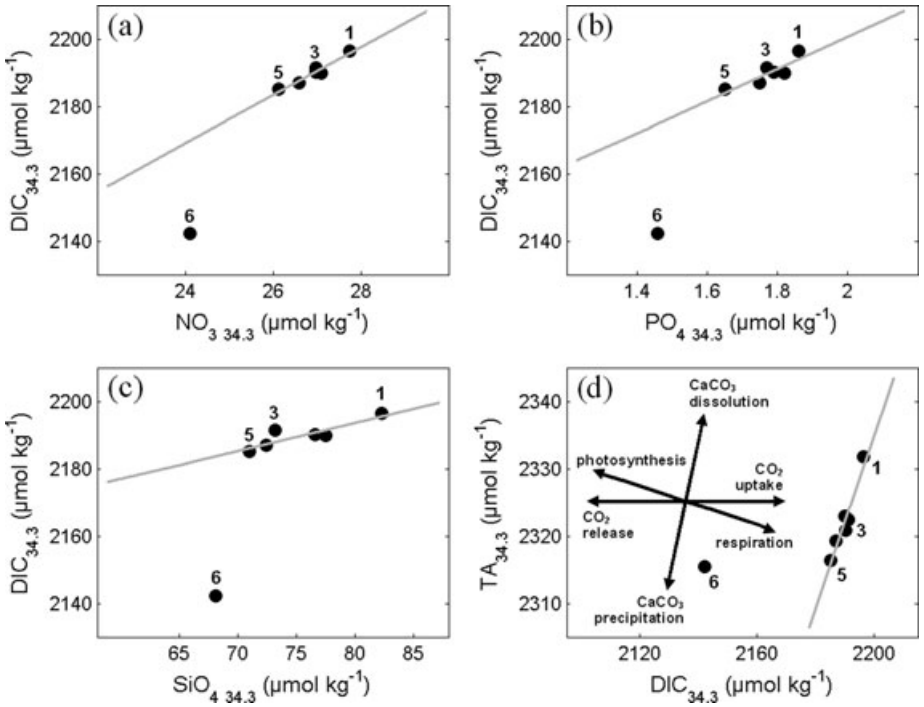

Fig. 5. Average summer mixed layer (stations 1, 3, 5 and 6) and underway salinity normalized DIC ($DIC_{34.3}$, μmol kg^{-1}) as a function of salinity normalized (a) nitrate ($NO_{334.3}$, μmol kg^{-1}), (b) phosphate ($PO_{434.3}$, μmol kg^{-1}), (c) silicate ($SiO_{434.3}$, μmol kg^{-1}) and (d) salinity normalized total alkalinity ($TA_{34.3}$, μmol kg^{-1}) as a function of $DIC_{34.3}$ (μmol kg^{-1}). The theoretical trends (d, insert) show the variation of $DIC_{34.3}$ and $TA_{34.3}$ with respect to certain biogeochemical processes, adapted from Zeebe and Wolf-Gladrow (2001). The trend lines represent the best fit from linear regression, excluding station 6.

suggests that samples from this location had either enriched DIC or depleted TA, or both, upon analysis. DIC increases occur from dissolution of carbonates, CO_2 uptake and remineralization of organic matter (Fig. 5d). Alkalinity deficits result from carbonate mineral precipitation and remineralization of organic matter. With respect to the high DIC_0 (Section 2.3), it is proposed that there is an additional source of DIC in the sea ice, such as bacterial degradation or the presence of labile organic matter. In the region of very recent ice melt, prior to biological assimilation, the 'extra' DIC would contribute to the observed fCO_2 offset.

4.2. Seasonal changes in carbonate chemistry

The depth of the winter mixed layer and temperature of the WW increased northwards from waters beneath sea ice to waters proximal to the ACC at 59°S (Table 2). Away from the region of greatest sea ice melt, WW salinity and concentrations of macronutrients, DIC and TA had little variation. North of the MIZ, the phytoplankton community was made up of cryptophytes and naked dinoflagellates (Korb et al., 2010), with the cryptophytes accounting for the elevated concentrations of chlorophyll-a north of the South Orkney Islands (Fig. 3f). This corresponded to the undersaturation in sea surface fCO_2 observed approaching the SB (north of station 10) and supports the idea of the frontal waters as an area of high productivity. In contrast, WW values of DIC and $DIC_{34.3}$ are relatively constant for nearly all stations and hence processes that affect DIC concentrations, either at the surface during the winter or through advection and slight vertical mixing in the winter mixed layer during the summer (Section 2.7), act uniformly across the Weddell–Scotia Confluence.

The seasonal change in carbonate chemistry can be explored by comparing $DIC_{34.3}$ and $TA_{34.3}$ at depth intervals from the surface to below the winter mixed layer (Fig. 6). Trends in $DIC_{34.3}$ and $TA_{34.3}$ in the summer mixed layer for stations located in the MIZ were explained previously (Section 4.1). Stations north of the MIZ, showed comparatively reduced DIC in the summer mixed layer at a narrow range of $TA_{34.3}$ of less than 10 μmol kg^{-1}. With the exception of station 11, surface $TA_{34.3}$ and $DIC_{34.3}$ for stations north of the MIZ tended to follow a 2:1 trend, but from a different starting point compared to the MIZ stations (Fig. 6a). As WW $DIC_{34.3}$ and $TA_{34.3}$ for all stations are quite similar (Fig. 6c), the greater $DIC_{34.3}$ deficit observed north of the MIZ is attributed to the greater photosynthetic activity that had occurred in the northern Weddell–Scotia Confluence, compared to the MIZ, by the summer.

Below the summer mixed layer, there was a gradual increase in $DIC_{34.3}$ and $TA_{34.3}$ throughout the water column for all stations (Fig. 6b). Values of $TA_{34.3}$ remained relatively constant compared to $DIC_{34.3}$ at all depths. This pattern indicates the influence of biological carbon uptake on summer

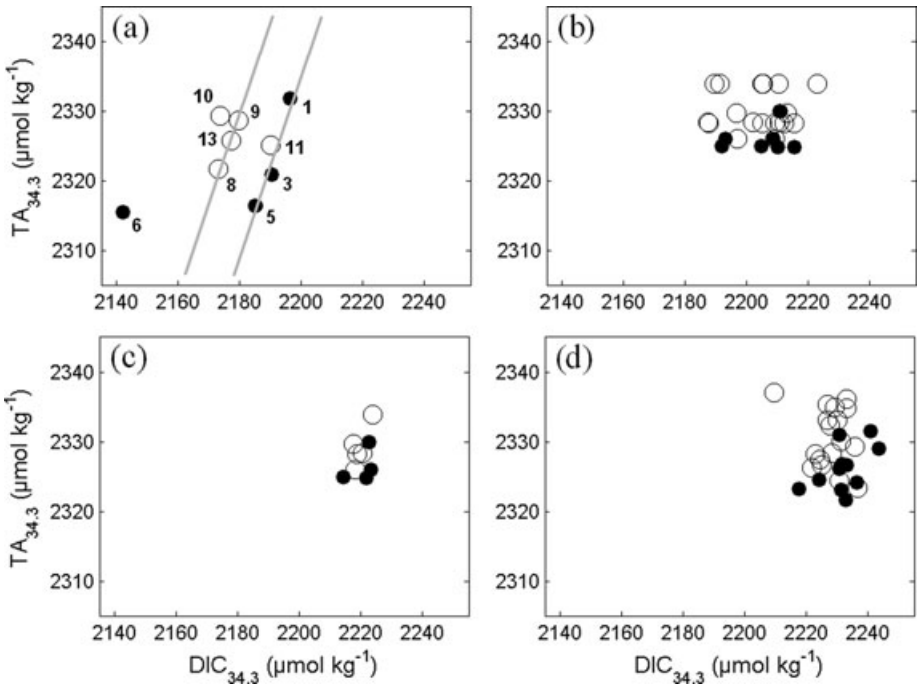

Fig. 6. Salinity normalized total alkalinity ($TA_{34.3}$, μmol kg^{-1}) as a function of salinity normalized dissolved inorganic carbon ($DIC_{34.3}$, μmol kg^{-1}) for all marginal ice zone (MIZ) stations (stations 1–6, filled circles) and stations north of the MIZ (stations 8–13, open circles) within (a) the summer mixed layer, (b) the transition between the summer and winter mixed layers, (c) the Winter Water at the θ_{min} and (d) below the θ_{min} to 200 m depth. The grey lines (a) are hypothetical trend lines with a 2:1 slope.

DIC concentrations (Fig. 5d) across the Weddell–Scotia Confluence.

Similarly to surface biogeochemical distributions, the principal exception to the WW trends was station 6, where salinity and the concentrations of macronutrients and DIC were the lowest observed for the whole Weddell–Scotia Confluence (Table 2). Vertical profiles at station 6 show a deflection below the winter mixed layer, at about 130 m, of relatively cold, fresh water (Fig. 4a). This corresponds to reduced DIC and macronutrient concentrations compared to station 5 (Figs 4d–f). This could be a result of the deep penetration of brines where biological activity has amplified the reduction in DIC. As station 6 is located over shallow topography, the interaction of water masses and bathymetry (Section 4.1) could enhance vertical mixing and potentially erode the winter mixed layer from below (Section 2.7). These results highlight the potential for overestimation of hydrographic and biogeochemical parameters in the WW, however this effect is estimated to be small (Section 2.7).

To further investigate the processes that affect the sea surface carbonate chemistry across the Weddell–Scotia Confluence during the summer, the seasonal depletion of inorganic carbon was determined for all stations, as detailed in Section 2.7 (Table 5).

Changes in salinity as a result of freshwater input accounted for between 14 and 32 $\pm$ 2 μmol kg^{-1} of the seasonal change for all stations (Table 5), highlighting the influence of sea ice melt on the carbonate chemistry of the Southern Ocean. The seasonal depletion in DIC due to the photosynthetic production of organic carbon showed a general northward increase, with prominent utilization of DIC in and around the receding ice edge and at the SB. This is in agreement with previous accounts of enhanced biological activity at these locations (Comiso et al., 1993; Helbling et al., 1993; Holm-Hansen and Hewes, 2004; Hewes et al., 2008). Surface waters for the whole region showed $TA_{34.3}$ and $DIC_{34.3}$ deficits characteristic of ikaite precipitation (Figs 5d and 6). For most stations this was strongly correlated to salinity, which suggests that continual sea ice melt and release of DIC- and TA-poor brines into the surface acts to rapidly change the carbonate chemistry of the Weddell–Scotia Confluence during summer sea ice melt. This was exemplified where the greatest extent of sea ice melt had occurred and an ice edge bloom had developed. Upper ocean distributions of DIC and TA showed a general decrease from waters beneath sea ice to the region of substantial sea ice melt and enhanced biological activity (Fig. 3). This culminated with the largest DIC deficits due to photosynthetic production of organic carbon and carbonate processes of 41 $\pm$ 1 and 12 $\pm$ 3 μmol kg^{-1}, respectively, and was accompanied by a strong drawdown of CO_2 (Fig. 2a). Following the same hypothesis, carbonate minerals in melting Nordic sea ice have been proposed to enhance the uptake of CO_2 during summer sea ice melt (Rysgaard et al., 2009).

The residual DIC changes are the result of other processes not previously assessed, such as CO_2 exchange. Large, positive

Table 5. The inorganic carbon budget for all stations from 62.61°S (station 1) to 59.14°S (station 13) as determined by eq. (3)

Station	$\Delta DIC_{deficit}$ (μmol kg^{-1})	$\Delta DIC_{salinity}$ (μmol kg^{-1})	$\Delta DICC_{org}$ (μmol kg^{-1})	$\Delta DICCaCO_3$ (μmol kg^{-1})	$\Delta DIC_{residual}$ (μmol kg^{-1})
1	-54 ± 2	-28 ± 2	-4 ± 6	2 ± 3	-24 ± 7
3	-57 ± 2	-24 ± 2	-19 ± 5	-7 ± 3	-7 ± 6
5	-63 ± 2	-24 ± 2	-36 ± 2	-8 ± 3	5 ± 5
6	-109 ± 2	-31 ± 2	-41 ± 1	-12 ± 3	-25 ± 4
8	-80 ± 2	-32 ± 2	-29 ± 8	-6 ± 3	-13 ± 9
9	-61 ± 2	-20 ± 2	-31 ± 5	-4 ± 3	-6 ± 6
10	-67 ± 2	-21 ± 2	-59 ± 6	-6 ± 3	19 ± 7
11	-54 ± 2	-21 ± 2	-59 ± 1	-8 ± 3	34 ± 4
13	-60 ± 2	-14 ± 2	-66 ± 9	-8 ± 3	28 ± 10

residuals north of the MIZ (Table 5) and ΔfCO_2 of about -30 μatm (Fig. 2a) suggest a sustained input of DIC through CO_2 uptake from the atmosphere. Based on in situ fCO_2, ΔfCO_2 and DIC measurements and Revelle factors between 13 and 15 (Revelle and Suess, 1957), atmospheric CO_2 uptake would act to increase DIC by 15–16 μmol kg^{-1} at stations 11 and 13. This could, in part, account for the residual DIC concentrations at the SB where longer duration, but lower magnitude, CO_2 uptake from the atmosphere is likely to occur in comparison with the larger, more transient sink of the MIZ. The large residuals could also imply limitations to the seasonal deficit technique, as previously discussed (Section 2.7).

4.3. Comparison to a surface water CO_2 climatology

The CO_2 sink of -0.06 Pg C yr^{-1}, between 62 and 52°S in the reference year 2000, is a result of an average ΔfCO_2 of -5 μatm, ranging from -15 μatm in January to 12 μatm in September (Takahashi et al., 2009). Data from the Weddell–Scotia Confluence (62.6–59.1°S) show that the region was dominated by CO_2 undersaturation at the sea surface, with an average ΔfCO_2 of -25 μatm (range from -95 to 14 μatm, Fig. 2a) during summer 2008. The potential CO_2 source of 14 μatm observed beneath the sea ice cover near station 1 is very similar to the ΔfCO_2 maximum from the climatology (12 μatm). The strong undersaturation of fCO_2 in the region of substantial sea ice melt far exceeded that of the climatology, by up to 80 μatm. In reference to the climatological ΔfCO_2 maximum of about 12 μatm, it is hypothesized that the Weddell–Scotia Confluence is a region of CO_2 uptake of greater than 0.06 Pg C yr^{-1}. However, investigations into the function of Antarctic sea ice as a permeable 'barrier' to CO_2 exchange may require these estimates to be re-evaluated (Nomura et al., 2006).

5. Conclusion

The precipitation of carbonate minerals such as ikaite in sea ice has the net effect of decreasing DIC and alkalinity and increasing the fCO_2 in the sea ice brine. Deficits in salinity normalized DIC and alkalinity observed in the summer mixed layer of the Weddell–Scotia Confluence are consistent with the release of brines from melting sea ice, where ikaite precipitation has taken place. Across the MIZ, ikaite precipitation accounted for up 12 ± 3 μmol kg^{-1}, or 13%, of the summer DIC deficit and was strongly correlated to the amount of sea ice melt that had taken place. Photosynthetic production of organic carbon had the largest effect on summer DIC concentrations, resulting in deficits of 41 ± 1 μmol kg^{-1} at the receding ice edge and 66 ± 9 μmol kg^{-1} at the SB. The effects of biological carbon uptake became superimposed on those of the sea ice carbonate chemistry, rapidly reducing fCO_2 compared to waters beneath the sea ice. These processes created substantial undersaturation in fCO_2 of 95 μatm in the MIZ during the summer thaw.

The 'sea ice CO_2 pump' hypothesis suggests that the dissolution of calcium carbonate minerals in meltwater during the summer promotes CO_2 uptake from the atmosphere. The carbonate chemistry data for the MIZ of the Weddell–Scotia Confluence suggest that it is the transfer of DIC- and TA-poor brines into the surface water during ice melt, in the presence of phytoplankton blooms, that drive a strong sink for CO_2 during the summer. Further work should be directed at improving the understanding of sea ice carbonate chemistry and its role in the sea ice carbon pump of the polar oceans.

6. Acknowledgments

The authors would like to thank the Captain, officers, crew and scientists involved in cruise JR177 and the British Antarctic Survey for making the RRS *James Clark Ross* available to us. The cruise was a component of the British Antarctic Survey's DISCOVERY-2010 programme. This work is part of PhD research by EM Jones at the University of East Anglia funded by the Natural Environment Research Council (NERC) under the auspices of the Centre for observation of Air-Sea Interactions and fluXes (CASIX) (NER/F14/G6/115). Participation in the cruise was supported by the Antarctic Funding Initiative (AFI)

through the Collaborative Gearing Scheme (CGS8/28). The authors acknowledge the constructive comments by the editors and an anonymous reviewer.

References

Ackley, S. F. and Sullivan, C. W. 1994. Physical controls on the development and characteristics of Antarctic sea-ice biological communities—a review and synthesis. *Deep-Sea Res. I* **41**, 1583–1604.

Alvarez, M., Rios, A. F. and Roson, G. 2002. Spatio-temporal variability of air-sea fluxes of carbon dioxide and oxygen in the Bransfield and Gerlache Straits during Austral summer 1995–96. *Deep-Sea Res. II* **49**, 643–662.

Anderson, L. A. and Sarmiento, J. L. 1994. Redfield Ratios of remineralization determined by nutrient data analysis. *Global Biogeochem. Cycle* **8**, 65–80.

Ardelan, M. V., Holm-Hansen, O., Hewes, C. D., Reiss, C. S., Silva, N. S. and co-authors. 2010. Natural iron enrichment around the Antarctic Peninsula in the Southern Ocean. *Biogeosciences* **7**, 11–25.

Bakker, D. C. E., de Baar, H. J. W. and Bathmann, U. V. 1997. Changes of carbon dioxide in surface waters during spring in the Southern Ocean. *Deep-Sea Res. II* **44**, 91–127.

Bakker, D.C.E., Hoppema, M., Schroder, M., Geibert, W. and de Baar, H. J. W. 2008. A rapid transition from ice covered CO_2-rich waters to a biologically mediated CO_2 sink in the eastern Weddell Gyre. *Biogeosciences* **5**, 1373–1386.

Bellerby, R. G. J., Hoppema, M., Fahrbach, E., de Baar, H. J. W. and Stoll, M. H. C. 2004. Interannual controls on Weddell Sea surface water fCO_2 during the autumn-winter transition phase. *Deep-Sea Res. I* **51**, 793–808.

Blain, S., Quéguiner, B., Armand, L., Belviso, S., Bombled, B. and co-authors. 2007. Effect of natural iron fertilization on carbon sequestration in the Southern Ocean. *Nature* **446**, 1070–1075.

Brainerd, K. E. and Gregg, M. C. 1995. Surface mixed and mixing layer depths. *Deep-Sea Res. I* **42**, 1521–1543.

Buma, A. G. J., Gieskes, W. W. C. and Thomsen, H. A. 1992. Abundance of cryptophyceae and chlorophyll b containing organisms in the Weddell–Scotia Confluence area in the spring of 1988. *Polar Biol.* **12**, 43–52.

Carmack, E. C. and Foster, T. D. 1975. Flow of water out of Weddell Sea. *Deep-Sea Res.* **22**, 711–724.

Ciattaglia, L., Colombo, T. and Masarie, K. A. 1999. Continuous measurements of atmospheric CO_2 at Jubany Station, Antarctica. *Tellus* **51B**, 713–721.

Comiso, J. C., McClain, C. R., Sullivan, C. W., Ryan, J. P. and Leonard, C. L. 1993. Coastal Zone Color Scanner pigment concentrations in the Southern Ocean and relationships to geophysical surface-features. *J. Geophys. Res.* **98**, 2419–2451.

de Baar, H. J. W., Buma, A. G. J., Nolting, R. F., Cadee, G. C., Jacques, G. and co-authors 1990. On iron limitation of the Southern Ocean – experimental observations in the Weddell and Scotia Seas. *Mar. Ecol. Progr. Ser.* **65**, 105–122.

Deacon, G. E. R. 1979. Weddell Gyre. *Deep-Sea Res.* **26**, 981–995.

Delille, B., Jourdain, B., Borges, A. V., Tison, J. L. and Delille, D. 2007. Biogas (CO_2, O_2, dimethylsulfide) dynamics in spring Antarctic fast ice. *Limnol. Oceanogr.* **52**, 1367–1379.

Dickson, A. G. and Millero, F. J. 1987. A comparison of the equilibrium constants for the dissociation of carbonic acid in seawater media. *Deep-Sea Res.* **34**, 1733–1743.

Dickson, A. G. 1981. An exact definition of total alkalinity and a procedure for the estimation of alkalinity and total inorganic carbon from titration data. *Deep-Sea Res.* **28**, 609–623.

DOE 2007. In: *Guide to Best Practices for Ocean CO_2 Measurements* (eds A.G. Dickson, C.L. Sabine and J.R. Christian). PICES Special Publication 3, 1–191.

Dieckmann, G. S., Nehrke, G., Papadimitriou S., Gottlicher, J., Steininger, R. and co-authors. 2008. Calcium carbonate as ikaite crystals in Antarctic sea ice. *Geophys. Res. Lett.*, **35**. doi:10.1029/2008GL033540.

Dulaiova, H., Ardelan, M. V., Henderson, P. B. and Charette, M. A. 2009. Shelf-derived iron inputs drive biological productivity in the southern Drake Passage. *Global Biogeochem. Cycle* **23**, doi:10.1029/2008GB003406.

Friis, K., Körtzinger, A. and Wallace, D. W. R. 2003. The salinity normalization of marine inorganic carbon chemistry data. *Geophys. Res. Lett.* **30**, doi:10.1029/2002GL015898.

GEBCO, 2001. *General Bathymetric Chart of the Oceans Digital Atlas*. British Oceanographic Data Centre, Liverpool, UK.

Gibson, J. A. E. and Trull, T. W. 1999. Annual cycle of fCO_2 under sea ice and in open water in Prydz Bay, east Antarctica. *Mar. Chem.* **66**, 187–200.

Gill, A. E. 1973. Circulation and bottom water production in Weddell Sea. *Deep-Sea Res.* **20**, 111–140.

Gleitz, M., Grossmann, S., Scharek, R. and Smetacek, V. 1996. Ecology of diatom and bacterial assemblages in water associated with melting summer sea ice in the Weddell Sea, Antarctica. *Antarct. Sci.* **8**, 135–146.

Gleitz, M., Vonderloeff, M. R., Thomas, D. N., Dieckmann, G. S. and Millero, F. J. 1995. Comparison of summer and winter inorganic carbon, oxygen and nutrient concentrations in Antarctic sea ice brine. *Mar. Chem.* **51**, 81–91.

Gouretski, V. V. and Danilov, A. I. 1993. Weddell Gyre – structure of the eastern boundary. *Deep-Sea Res. I* **40**, 561–582.

Heinze, C., Maier-Reimer E. and Winn, K. 1991. Glacial pCO_2 reduction by the World Ocean: experiements with the Hamburg carbon cycle model. *Paleoceanography*. **6**, 395–430.

Helbling, E. W., Amos, A. F., Silva, N., Villafane, V. and Holm-Hansen, O. 1993. Phytoplankton distribution and abundance as related to a frontal system north of Elephant Island, Antarctica. *Antarct. Sci.* **5**, 25–36.

Hewes, C. D., Reiss, C. S., Kahru, M., Mitchell, B. G. and Holm-Hansen, O. 2008. Control of phytoplankton biomass by dilution and mixed layer depth in the western Weddell–Scotia Confluence. *Mar. Ecol. Prog. Ser.* **366**, 15–29.

Holm-Hansen, O. and Hewes, C. D. 2004. Deep chlorophyll-a maxima (DCMs) in Antarctic waters—I. relationships between DCMs and the physical, chemical, and optical conditions in the upper water column. *Polar Biology* **27**, 699–710.

Holm-Hansen, O. and Mitchell, B. G. 1991. Spatial and temporal distribution of phytoplankton and primary production in the western Bransfield Strait region. *Deep-Sea Res. A* **38**, 961–980.

Hoppema, M., de Baar, H. J. W., Fahrbach, E., Hellmer, H. H. and Klein, B. 2003. Substantial advective iron loss diminishes phytoplankton

production in the Antarctic Zone. *Global Biogeochem. Cycle.* **17**, doi:10.1029/2002GB001957.

Hoppema, M., Fahrbach, E., Schroder, M., Wisotzki, A. and de Baar, H. J. W. 1995. Winter-summer differences of carbon dioxide and oxygen in the Weddell Sea surface layer. *Mar. Chem.* **51**, 177–192.

Hoppema, M., Fahrbach, E., Stoll, M. H. C. and de Baar, H. J. W. 1999. Annual uptake of atmospheric CO_2 by the Weddell Sea derived from a surface layer balance, including estimations of entrainment and new production. *J. Mar. Sys.* **19**, 219–233.

Hoppema, M., Stoll, M. H. C. and de Baar, H. J. W. 2000. CO_2 in the Weddell Gyre and Antarctic Circumpolar Current: austral autumn and early winter. *Mar. Chem.* **72**, 203–220.

Ishii, M., Inoue, H. Y. and Matsueda, H. 2002. Net community production in the marginal ice zone and its importance for the variability of the oceanic pCO_2 in the Southern Ocean south of Australia. *Deep-Sea Res. II* **49**, 1691–1706.

Ishii, M., Inoue, H.Y., Matsueda, H. and Tanoue, E. 1998. Close coupling between seasonal biological production and dynamics of dissolved inorganic carbon in the Indian Ocean sector and the western Pacific Ocean sector of the Antarctic Ocean. *Deep-Sea Res. I* **45**, 1187–1209.

Jacques, G. and Panouse, M. 1991. Biomass and composition of size fractionated phytoplankton in the Weddell–Scotia Confluence area. *Polar Biol.* **11**, 315–328.

Jennings, J. C., Gordon, L. I. and Nelson, D. M. 1984. Nutrient depletion indicates high primary productivity in the Weddell Sea. *Nature* **309**, 51–54.

Jouandet, M. P., Blain, S., Metzl, N., Brunet, C., Trull, T. W. and co-authors 2008. A seasonal carbon budget for a naturally iron-fertilised bloom over the Kerguelen Plateau in the Southern Ocean. *Deep-Sea Res. II* **55**, 856–867.

Johnson, K. M., Sieburth, J. M., Williams, P. J. L. and Brandstrom, L. 1987. Coulometric total carbon dioxide analysis for marine studies—automation and calibration. *Mar. Chem.* **21**, 117–133.

Kang, S. H., Kang, J. S., Lee, S., Chung, K. H., Kim, D. and co-authors 2001. Antarctic phytoplankton assemblages in the marginal ice zone of the northwestern Weddell Sea. *J. Plankton Res.* **23**, 333–352.

Klatt, O., Roether, W., Hoppema, M., Bulsiewicz, K., Fleischmann, U. and co-authors. 2002. Repeated CFC sections at the Greenwich Meridian in the Weddell Sea. *J. Geophys. Res.* **107**, doi:10.1029/2000JC000731.

Korb, R. E., Whitehouse, M. J., Thorpe, S. E. and Gordon, M. 2005. Primary production across the Scotia Sea in relation to the physico-chemical environment. *J. Mar. Sys.* **57**, 231–249.

Korb, R. E., Whitehouse, M. J., Gordon, M., Ward, P. and Poulton, A.J. 2010. Summer microplankton community structure across the Scotia Sea: implications for biological carbon export. *Biogeosciences* **7**, 343–356.

Krembs, C. and Engel, A. 2001. Abundance and variability of microorganisms and transparent exopolymer particles across the ice-water interface of melting first-year sea ice in the Laptev Sea (Arctic). *Mar. Biol.* **138**, 173–185.

Lancelot, C., Mathot, S., Veth, C. and Debaar, H. 1993. Factors controlling phytoplankton ice edge blooms in the Marginal Ice Zone of the northwestern Weddell Sea during sea ice retreat 1988 – field observations and mathematical modelling. *Polar Biol.* **13**, 377–387.

Lannuzel, D., Schoemann, V., de Jong, J., Chou, L., Delille, B. and co-authors. 2008. Iron study during a time series in the western Weddell pack ice. *Mar. Chem.* **108**, 85–95.

Lannuzel, D., Schoemann, V., de Jong, J., Tison, J. L. and Chou, L. 2007. Distribution and biogeochemical behaviour of iron in the East Antarctic sea ice. *Mar. Chem.* **106**, 18–32.

Lewis, E. and Wallace, D. W. R. 1998. CO2SYS-Program developed for the CO_2 system calculations. *Carbon Dioxide Inf. Anal. Centre*. Report ORNL/CDIAC-105.

Löscher, B. M., de Baar, H. J. W., de Jong, J. T. M., Veth, C. and Dehairs, F. 1997. The distribution of Fe in the Antarctic Circumpolar Current. *Deep-Sea Res. II* **44**, 143–187.

Marion, G. M. 2001. Carbonate mineral solubility at low temperatures in the Na-K-Mg-Ca-H-Cl-SO_4-OH-HCO_3-CO_3-CO_2-H_2O system. *Geochim. Cosmochim. Acta* **65**, 1883–1896.

Martin, J. H. 1990. Glacial-interglacial CO_2 change: the iron hypothesis. *Paleoceanography* **5**, 1–13.

Mehrbach, C., Culberson, C. H., Hawley, J. E. and Pytkowicz, R. M. 1973. Measurement of the apparent dissociation constants of carbonic acid in seawater at atmospheric pressure. *Limnol. Oceanogr.* **18**, 897–907.

Meiners, K. M., Papadimitriou, S., Thomas, D. N., Norman, L. and Dieckmann, G. S. 2009. Biogeochemical conditions and ice algal photosynthetic parameters in Weddell Sea ice during early spring. *Polar Biol.* **32**, 1055–1065.

Minas, H. J. and Minas, M. 1992. Net community production in high nutrient-low chlorophyll waters of the tropical and Antarctic Oceans – grazing vs iron hypothesis. *Oceanol. Acta* **15**, 145–162.

Naveira Garabato, A. C., Heywood, K. J. and Stevens, D. P. 2002. Modification and pathways of Southern Ocean Deep Waters in the Scotia Sea. *Deep-Sea Res. I* **49**, 681–705.

Nomura, D., Inoue, H. Y. and Yoyota T. 2006. The effect of sea-ice growth on air-sea CO_2 flux in a tank experiment. *Tellus* **58B**, 418–426.

Nolting, R. F., de Baar, H. J. W., Vanbennekom, A. J. and Masson, A. 1991. Cadmium, copper and iron in the Scotia Sea, Weddell Sea and Weddell Scotia Confluence (Antarctica). *Mar. Chem.* **35**, 219–243.

Orsi, A. H., Johnson, G. C. and Bullister, J. L. 1999. Circulation, mixing, and production of Antarctic Bottom Water. *Progr. Oceanogr.* **43**, 55–109.

Orsi, A. H., Whitworth, T. and Nowlin, W. D. 1995. On the meridional extent and fronts of the Antarctic Circumpolar Current. *Deep-Sea Res. I* **42**, 641–673.

Papadimitriou, S., Kennedy, H., Kattner, G., Dieckmann, G. S. and Thomas, D. N. 2004. Experimental evidence for carbonate precipitation and CO_2 degassing during sea ice formation. *Geochim. Cosmochim. Acta* **68**, 1749–1761.

Papadimitriou, S., Thomas, D. N., Kennedy, H., Haas, C., Kuosa, F. and co-authors. 2007. Biogeochemical composition of natural sea ice brines from the Weddell Sea during early austral summer. *Limnol. Oceanogr.* **52**, 1809–1823.

Parsons, T. R., Maita, Y., Lalli, C. M. 1984. *A Manual of Chemical and Biological Methods for Seawater Analysis*. Pergamon Press, Oxford, 1–173.

Patterson, S. L. and Sievers, H. A. 1980. The Weddell–Scotia Confluence. *J. Phys. Oceanogr.* **10**, 1584–1610.

Pollard, R. T., Lucas, M. I. and Read, J. F. 2002. Physical controls on biogeochemical zonation in the Southern Ocean. *Deep-Sea Res. II* **49**, 3289–3305.

Pondaven, P., Ragueneau, O., Tréguer, P., Hauvespre, A., Dezileua, L. and co-authors. 2000. Resolving the 'opal paradox' in the Southern Ocean. *Nature* **405**, 168–172.

Redfield, A. C., Ketchum, B. H. and Richards, F. A. 1963. The influence of organisms on the composition of seawater. In: *The Sea. Vol. 2. The Composition of Seawater* (ed. M.N. Hill). Wiley, New York, 26–77.

Revelle, R. and Suess, H. E. 1957. Carbon dioxide exchange between atmosphere and ocean and the question of an increase of atmospheric CO_2 during the past decades. *Tellus* **9**, 18–27.

Rintoul, S. R. and Sokolov, S. 2001. Baroclinic transport variability of the Antarctic Circumpolar Current south of Australia (WOCE repeat section SR3). *J. Geophys. Res.* **106**, 2815–2832.

Rubin, S. I., Takahashi, T., Chipman, D. W. and Goddard, J. G. 1998. Primary productivity and nutrient utilization ratios in the Pacific sector of the Southern Ocean based on seasonal changes in seawater chemistry. *Deep-Sea Res. I* **45**, 1211–1234.

Rysgaard, S., Glud, R. N., Sejr, M. K., Bendtsen, J. and Christensen, P. B. 2007. Inorganic carbon transport during sea ice growth and decay: a carbon pump in polar seas. *J. Geophys. Res.* **112**, doi:10.1029/2006JC003572.

Rysgaard, S., Bendtsen, J., Pedersen, L. T., Ramlov, H. and Glud, R. N. 2009. Increased CO_2 uptake due to sea ice growth and decay in Nordic Seas. *J. Geophys. Res.* **114**, doi:10.1029/2008JC005088.

Sakshaug, E., Slagstad, D. and Holm-Hansen, O. 1991. Factors controlling the development of phytoplankton blooms in the Antarctic Ocean – a mathematical model. *Mar. Chem.* **35**, 259–271.

Sanudo-Wilhelmy, S. A., Olsen, K. A., Scelfo, J. M., Foster, T. D. and Flegal, A. R. 2002. Trace metal distributions off the Antarctic Peninsula in the Weddell Sea. *Mar. Chem.* **77**, 157–170.

Schroder, M. and Fahrbach, E. 1999. On the structure and the transport of the eastern Weddell Gyre. *Deep-Sea Res. II* **46**, 501–527.

Schuster, U. and Watson, A. J. 2007. A variable and decreasing sink for atmospheric CO_2 in the North Atlantic. *J. Geophys. Res.* **112**, doi:10.1029/2006JC003941.

Sedwick, P. N. and DiTullio, G. R. 1997. Regulation of algal blooms in Antarctic shelf waters by the release of iron from melting sea ice. *Geophys. Res. Lett.* **24**, 2515–2518.

Shim, J., Kang, Y. C., Kim, D. and Choi, S.-H. 2006. Distribution of net community production and surface pCO_2 in the Scotia Sea, Antarctica, during austral spring 2001. *Mar. Chem.* **101**, 68–84.

Sievers, H. A. and Nowlin, W. D. 1984. The stratification and water masses at Drake Passage. *J. Geophys. Res.* **89**, 489–514.

Smith, W. O. and Nelson, D. M. 1985. Phytoplankton bloom produced by a receding ice edge in the Ross Sea—spatial coherence with the density field. *Science* **227**, 163–166.

Smith, W. O. and Nelson, D. M. 1986. Importance of ice edge phytoplankton production in the Southern Ocean. *Bioscience* **36**, 251–257.

Stark, J. D., Donlon, C. J., Martin, M. J. and McCulloch, M. E. 2007. OSTIA: an operational, high resolution, real time, global sea surface temperature analysis system. In: *Marine Challenges: Coastline to Deep Sea*. Conference proceedings. Oceans '07 IEEE Aberdeen.

Stoll, M. H. C., de Baar, H. J. W., Hoppema, M. and Fahrbach, E. 1999. New early winter fCO_2 data reveal continuous uptake of CO_2 by the Weddell Sea. *Tellus* **51B**, 679–687.

Stoll, M. H. C., Thomas, H., de Baar, H. J. W., Zondervan, I., de Jong, E. and co-authors. 2002. Biological versus physical processes as drivers of large oscillations of the air-sea CO_2 flux in the Antarctic marginal ice zone during summer. *Deep-Sea Res. I* **49**, 1651–1667.

Sweeney, C., Smith, W. O., Hales, B., Bidigare, R. R., Carlson, C. A. and co-authors. 2000. Nutrient and carbon removal ratios and fluxes in the Ross Sea, Antarctica. *Deep-Sea Res. II* **47**, 3395–3421.

Takahashi, T., Olafsson, J., Goddard, J. G., Chipman, D. W. and Sutherland, S. C. 1993. Seasonal variation of CO_2 and nutrients in the high latitude surface oceans—a comparative-Study. *Global Biogeochem. Cycle* **7**, 843–878.

Takahashi, T., Sutherland, S. C., Wanninkhof, R., Sweeney, C., Feely, R. A. and co-authors. 2009. Climatological mean and decadal change in surface ocean pCO_2, and net sea-air CO_2 flux over the global oceans. *Deep-Sea Res. II* **56**, 554–577.

Tynan, C. T. 1998. Ecological importance of the Southern Boundary of the Antarctic Circumpolar Current. *Nature* **392**, 708–710.

Weiss, R. F., Ostlund, H. G. and Craig, H. 1979. Geochemical studies of the Weddell Sea. *Deep-Sea Res.* **26**, 1093–1120.

Whitehouse, M. J., 1997. *Automated Seawater Nutrient Chemistry*. British Antarctic Survey, Cambridge, 1–14.

Whitehouse, M. J., Korb, R. E., Atkinson, A., Thorpe, S. E. and Gordon, M. 2008. Formation, transport and decay of an intense phytoplankton bloom within the high-nutrient low-chlorophyll belt of the Southern Ocean. *J. Mar. Sys.* **70**, 150–167.

Whitworth, T. and Nowlin, W. D. 1987. Water masses and currents of the Southern Ocean at the Greenwich Meridian. *J. Geophys. Res.* **92**, 6462–6476.

Whitworth, T., Nowlin, W. D., Orsi, A. H., Locarnini, R. A. and Smith, S. G. 1994. Weddell Sea shelf water in the Bransfield Strait and Weddell–Scotia Confluence. *Deep-Sea Res. I* **41**, 629–641.

Zeebe, R. E. and Wolf-Gladrow, D. A. 2001. Equilibrium. In: *CO_2 in Seawater: Equilibrium, Kinetics, Isotopes* (ed. D. Halpern). Elsevier, Amsterdam, 1–83.